# Advancements in the Search for Superhard Ultra-Incompressible Metal Borides

By *Jonathan B. Levine, Sarah H. Tolbert,** and *Richard B. Kaner**

This article is dedicated in memory of Professor John J. Gilman, whose creativity and inspiration were instrumental in our efforts to develop ultra-incompressible, superhard borides.

**Dense transition metal borides have recently been identified as superhard materials that offer the possibility of ambient pressure synthesis compared to the conventional high pressure, high temperature approach. This feature article begins with a discussion of the relevant physical properties for this class of compounds, followed by a summary of the synthesis and properties of several transition metal borides. A strong emphasis is placed on correlating mechanical properties with electronic and atomic structure of these materials in an effort to better predict new superhard compounds. It concludes with a perspective of future research directions, highlighting some recent results and presenting several new ideas that remain to be tested.**

## 1. Introduction

The search for new ultra-incompressible, superhard materials with mechanical properties that rival those of diamond continues to be an exciting and active area of research.[1–3] Such new materials are extremely useful as abrasives, cutting tools, and coatings because of both the inability of diamond to effectively cut ferrous materials and the high cost of synthesizing diamond or diamond substitutes, such as cubic boron nitride (c-BN). Both diamond and c-BN must be synthesized under high pressure and high temperature (HPHT) conditions.

[*] Prof. S. H. Tolbert, Prof. R. B. Kaner, Dr. J. B. Levine[+]
Department of Chemistry and Biochemistry
UCLA
Los Angeles, CA 90095 (USA)
E-mail: tolbert@chem.ucla.edu; kaner@chem.ucla.edu
Prof. S. H. Tolbert, Prof. R. B. Kaner, Dr. J. B. Levine
California NanoSystems Institute
UCLA
Los Angeles, CA 90095 (USA)
Prof. R. B. Kaner
Department of Materials Science and Engineering
UCLA
Los Angeles, CA 90095 (USA)

[+] Current address: Rubicon Technology, Franklin Park, IL 60131, USA

**DOI: 10.1002/adfm.200901257**

Several recent reviews in the literature cover various aspects of this research field, including HPHT synthesis of superhard materials, superhard thin films and nanocomposites, and the ultimate goal of creating new bulk materials harder than diamond.[4–7] Progress is steadily being made in HPHT synthesis, where recent developments include the synthesis of diamond-like carbon, aggregate diamond nanorods, ultrahard fullerites, and boron nitride nanocomposites using pressures up to 20 GPa and temperatures approaching 2 000 °C. All of these materials possess hardness and bulk moduli values comparable to single-crystal diamond.[8–11]

In the present Feature Article, we limit our discussion to recent discoveries on the properties of dense transition metal borides in the continued search for new superhard materials. Note that the goal of this research is not to create a material harder than diamond, but rather to engineer a material that is superhard and can be easily synthesized in bulk quantities under non-HPHT conditions. New materials that can be produced in large quantities may enable new industrial applications, including improvements in cutting tools and wear-resistant coatings.

In order to systematically create new superhard phases (hardness $> 40$ GPa),[12] it is necessary to first understand the underlying phenomena that lead to such robust mechanical properties.[3] The mechanical properties of a material can be characterized in various ways and there exists no single method to determine the absolute strength of a material. Fundamentally, external forces applied to a solid material can cause translations or rotations, or they can induce stresses to produce strain in the material. These strains are manifested as volume changes, shape changes, and rotational changes. Stress and strain tensors are expressed in terms of the elastic stiffness constants, $C_{ij}$, of the material. The magnitude of each elastic constant increases as a solid's resistance to elastic deformation increases.[13] With knowledge of the elastic constants, the degree of elastic (reversible) deformation a material undergoes when subjected to stress can be understood. As these elastic deformations can often be correlated with plastic (irreversible) deformations, knowledge of the elastic stiffness constants is useful in understanding a material's strength. In order to properly characterize the material's response,

the orientation of the specimen must be known because the plastic and elastic deformations can manifest themselves along the direction of the applied stress, perpendicular to it, or some vector combination of the two directions. Ideally, superhard materials should be isotropic, otherwise they will preferentially deform in a specific direction.[14]

The measurement of a material's response to stress can be performed macroscopically, microscopically, or atomically, and the chosen scale will have a direct impact on the properties that are measured. Glass, for example, has very strong chemical bonds between silicon and oxygen, but it is prone to cracking (i.e., it is brittle), and is therefore not considered to be a very strong material.[13] In order to minimize the ambiguity associated with the meaning of ''strength'', emphasis here is placed on the bulk modulus as a measure of elastic (reversible) strength and the indentation hardness as a measure of plastic (irreversible) strength. Before an in-depth discussion on superhard borides, a brief description of these properties is given to clarify any misconceptions that may exist. For example, the mixing of the concepts of hardness and bulk modulus (i.e., stiffness) can be found in the article ''Osmium is not harder than diamond''.[15]

## 2. Mechanical Properties

Elastic stiffness, or incompressibility, is directly dependent on the elastic coefficients of a solid and it is commonly quantified by the bulk modulus, i.e., the resistance of a solid to volume compression under hydrostatic stress. Bulk modulus can be formally defined according to Equation 1:

$$B = -V\partial p/\partial V \quad (1)$$

where $p$ is the pressure, $V$ is the volume, and $\partial p/\partial V$ is the partial derivative of pressure with respect to volume. Bulk modulus is thus simply the inverse of the fractional volume change with pressure. Originally, the bulk modulus was shown to be strongly correlated with the molar volume ($V_m$) and cohesive energy ($E_c$) according to the relationship:

$$B \propto E_c/V_m \quad (2)$$

Elements with small molar volumes and strong interatomic forces resulting from high cohesive energies tend to have high bulk moduli.[4]

A survey of bulk moduli and cohesive energies as a function of atomic number is presented in Figure 1.[3,4] The natural logarithms of the bulk moduli are plotted in order to display a greater range in the variation of elastic stiffness on a single graph. Note the similarities between the peaks and valleys for both the bulk modulus and cohesive energy that roughly depend on the periodicity of the elements with half-filled shells exhibiting maxima for both terms. More recently, a clear correlation was shown between bulk modulus and valence electron density (VED—electrons/unit volume) because higher concentrations of electrons result in greater repulsive forces within the material.[3,16] Because the electron density is used rather than just the valence electron count, the favorable effects of decreasing atomic volume is already taken into account. Thus, VED provides a rudimentary gauge in the search for potentially new superhard materials given that superhard materials must be incompressible (as discussed below).

While bulk modulus measures the resistance to volume change for a constant shape, shear modulus measures the resistance to shape change at a constant volume. The shear modulus depends

**Jonathan B. Levine** is a solid state chemist who earned his Ph.D. in inorganic chemistry with a focus on superhard borides. He received his bachelor's degree in chemistry from Princeton University in 2004 and his Ph.D. from UCLA in 2009. After a postdoctoral appointment in Prof. Kaner's lab he began work as a crystal growth engineer for Rubicon Technology (Franklin Park, IL) where he is currently employed.

**Sarah H. Tolbert** is Professor of Chemistry and member of the California NanoSystems Institute at UCLA. After a Ph.D. at UC Berkeley and postdoctoral research at UC Santa Barbara, she joined UCLA in 1997 as an Assistant Professor and became a full Professor in 2006. Her research focuses on the chemistry and physics of novel materials, including superhard and ultra-incompressible borides, templated nanoporous frameworks, self-assembled semiconducting polymers, and organized nanocrystal arrays.

**Richard B. Kaner** is Professor of Chemistry, Professor of Materials Science and Engineering, and Associate Director of the California NanoSystems Institute at UCLA. After a Ph.D. at the University of Pennsylvania and postdoctoral research at UC Berkeley, he joined UCLA in 1987 as an Assistant Professor and became a full Professor in 1993. His research focuses on new routes to refractory materials including ultra-incompressible, superhard borides, conducting polymer nanofibers, and nanostructured carbon.

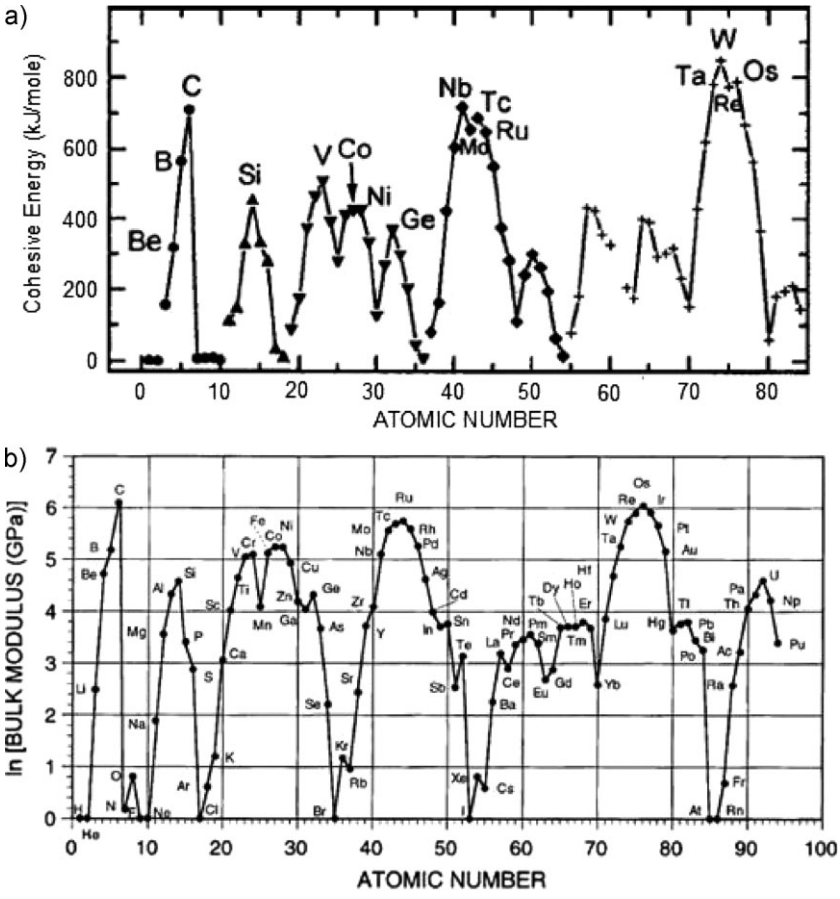


**Figure 1.** a) Cohesive energy as a function of atomic number (reproduced with permission from Ref. [4], copyright 2001 Taylor & Francis Ltd.), b) natural logarithm of the bulk modulus as a function of atomic number (reproduced from Ref. [3], copyright 2006 Elsevier). Both properties follow similar trends within the periodic table.

on both the plane of shear and the direction of shear, thus making it a more complex property than bulk modulus. Formally, the shear modulus, $G$, is defined as the ratio of shear stress to shear strain:

$$G = \frac{\text{stress}}{\text{strain}} = \frac{F/A}{\Delta x/L} \tag{3}$$

where $F$ is the applied force, $\Delta x$ is the resulting displacement, $A$ is the area upon which the force acts, and $L$ is the initial length. The higher the shear modulus, the greater the ability for a material to resist shearing forces and therefore, the more rigid the material is. For an isotropic system the shear modulus can be directly related to the bulk modulus, $B$, according to Equation 4:

$$G = \frac{3}{2} B \frac{1 - 2\nu}{1 + \nu} \tag{4}$$

where $\nu$ is the Poisson's ratio, that is, the value of the ratio of the transverse (contraction) strain to the corresponding axial (extension) strain of a material.[17] According to Equation 4, a high value for the shear modulus necessitates a large value for the bulk modulus and a small Poisson's ratio. A typical value for the Poisson's ratio is 0.1 for covalent materials and 0.3 for metallic materials.[14] A low Poisson's ratio results from directional bonds, which increase the shear modulus and limit the motion of dislocations, thereby increasing a material's hardness.

In contrast to the two types of elastic deformations discussed above, a material is hard if it resists plastic deformation.[2] This involves preventing the nucleation and motion of dislocations, an irreversible change in the structure, and is related to both elastic and plastic processes within a solid. A system with short covalent bonds tends to minimize such dislocations and a system with more delocalized bonding allows them.[18] Thus, diamond, containing covalent carbon–carbon bonds that are highly directional and very strong, is the hardest known material. Conversely, metals with their ''sea of electrons'' have non-directional metallic bonds and are generally soft and ductile.

In an effort to efficiently predict new superhard materials, relationships have been drawn between hardness and various elastic properties.[2,13,18,19] Previously, bulk modulus was thought to be a good predictor of hardness.[14] Although it is true that a hard material must have a high bulk modulus, it is a common misconception to believe that the inverse is true, that is, a material which is incompressible is hard. Osmium, for example, has a bulk modulus comparable to diamond, making it one of the most incompressible materials known.[20–23] The hardness of osmium, however, is within the range of other transition metals and is nearly two orders of magnitude lower than that of diamond, consistent with the non-directional nature of its delocalized electrons. The case of osmium exemplifies the drawback of using bulk modulus as an indicator of hardness. Bulk modulus is mainly dependent on the electron density and molar volume irrespective of the bond type or degree of ionicity. Thus, highly covalent materials and ionic or metallic materials can have similarly high bulk moduli resulting from high VEDs, even though their hardness values are substantially different.

Shear modulus provides a much better correlation with hardness than bulk modulus.[3,4,18,24] Covalent materials generally display high bond-bending force constants, contain highly directional bonds, and generally have high shear moduli. In an ionic material, however, the electrostatic interactions are omnidirectional, resulting in low bond-bending force constants and consequently a low shear modulus. Thinking back to hardness, dislocation motion requires atoms to move past each other. While this motion is plastic, rather than elastic, the actual atomic motions are much more closely related to those associated with shear, rather than volume compression. The shear modulus is therefore strongly correlated with hardness and provides the link between elastic properties and high hardness.[14,25] As a result, in contrast to

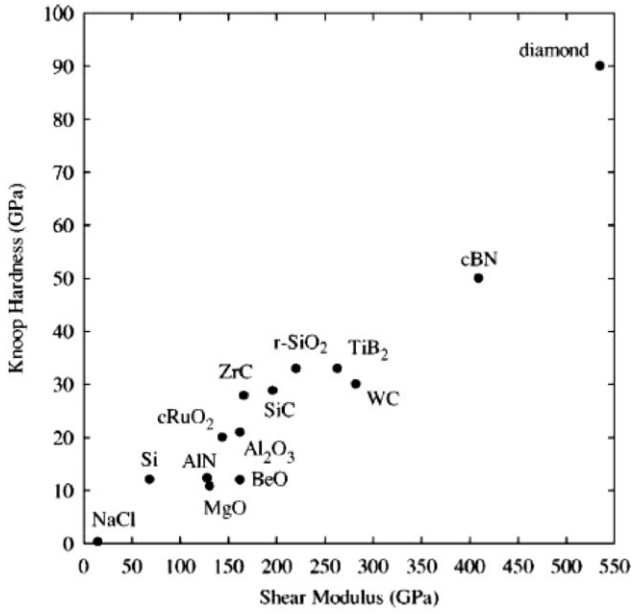


**Figure 2.** Hardness as a function of shear modulus for various covalent, ionic, and metallic materials. Reproduced with permission from the Annual Review of Materials Research, Ref. [14], copyright 2001 Annual Reviews.

the example given above for bulk moduli, even if an ionic and a covalent material possess equivalent bulk moduli, their shear moduli will differ substantially. The shear modulus is therefore a more accurate predictor of superhard materials and the correlation between hardness and shear modulus can be seen in Figure 2 for various covalent, ionic, and metallic materials.[14]

## 3. Conventional Superhard Materials

Diamond is generally regarded as the hardest bulk material with a measured hardness between 70 and 100 GPa depending on the type and quality of the diamond.[26] Diamond also possesses an extremely high shear modulus (534 GPa), the highest known bulk modulus (442 GPa), a very low Poisson's ratio (0.07), and a high thermal conductivity (20 W $cm^{-1}$ $K^{-1}$).[13,14,27,28] Diamond's exceptional hardness and shear strength originate from its crystal structure and the nature of its chemical bonds. Diamond crystallizes in a face-centered cubic lattice with one half of the tetrahedral sites filled. Every carbon atom is $sp^3$ hybridized with an interatomic distance of 1.54 Å. The strength and directionality of covalent carbon–carbon bonds limits the propagation of defects, which in turn resists plastic deformation, giving rise to the exceptional hardness of diamond. Diamond's phenomenal incompressibility can be correlated to its low molar volume and correspondingly high valence electron density. Due to the small size of each carbon atom, diamond has the highest VED of any known material (0.705 electrons $Å^{-3}$). When diamond is compressed elastically and isostatically, the energetically unfavorable electronic repulsions result in the highest measured bulk modulus (442 GPa).[27]

Diamond was first prepared synthetically in 1955 at the General Electric Company (GE) by Bundy et al. under 9.8 GPa of pressure at 2 300 °C.[29] This process has since been improved using different presses and the addition of catalysts in order to decrease the reaction conditions to approximately 5 GPa and 1 200 °C.[30] Diamond has traditionally been considered the best option for superhard industrial requirements and the current production of synthetic diamond is estimated to be 110 tons annually (500 million carats). Its mechanical robustness and general chemical inertness make it widely applicable. However, there are situations where materials with different chemical compositions would be better suited than diamond. For example diamond cannot be used to cut steel because the formation of iron carbide is thermodynamically favorable at elevated temperatures.

Since the 1950s, HPHT approaches to synthesizing new superhard materials have primarily focused on using the p-block elements. Light elements such as B, C, N, and O have been combined to make compounds with short, strong covalent bonds. By replacing every two carbon atoms in diamond with one boron atom and one nitrogen atom, a compound isoelectronic with diamond is created. This compound, known as cubic boron nitride (c-BN), was first synthesized at GE shortly after the synthesis of diamond.[31] Although c-BN is superhard, the slight decrease in covalency for B−N bonds compared to C−C bonds is enough to reduce the hardness from 100 GPa down to ~45 GPa.[32] Cubic boron nitride is not found in nature and can only be synthesized under high pressures (between 5 and 8 GPa) and temperatures (~1 800 °C).[31,32] Its insolubility in iron and other metal alloys makes it more useful for some industrial applications than diamond. Other superhard materials such as $B_6O$ and c-$BC_2N$ have since been synthesized under HPHT conditions; however, due to the need for extreme pressures (25 GPa for c-$BC_2N$) and temperatures, sample sizes are often limited to milligram quantities.[32–35]

One material that deserves a brief mention is $C_3N_4$. This compound, which is isostructural with $Si_3N_4$ (both α and β phases), was predicted to be superhard in 1984.[36,37] Sung and Sung calculated the structure of this theoretical compound and determined that the C−N bond distance would be 1.47 Å, 5% shorter than the C−C bond length in diamond.[37] With such a short bond length it was theorized that if this material could be synthesized it would be less compressible and likely harder than diamond.[38] Despite two decades pursuing this compound, no bulk sample of $C_3N_4$ has ever been produce to confirm the hardness predictions. Thus, there remains a need for a scalable, alternative route to produce new superhard phases that combine high hardness with chemical inertness and low-cost synthesis to yield practical benefits.

## 4. New Design Parameters Using Incompressible Transition Metals

A new method to creating ultra-incompressible hard materials, recently pioneered by our group, involves reacting light p-block elements with dense transition metals.[2] The benefit of using metals stems from the high valence electron densities for the 5 d metals[13] and high heats of formation of the respective borides, carbides, and oxides.[17,39] The obvious problem with metals is that metallic bonding is essentially omni-directional and therefore does a poor job of resisting either plastic or elastic shape deformations resulting in both a low shear modulus and low

hardness.[2] However, through the introduction of nonmetallic elements such as boron, carbon, nitrogen, or oxygen, covalent bonds to metals are formed that can drastically increase the hardness. Additionally, due to the high heats of formation, HPHT methods are unnecessary and low pressure solid state synthetic techniques can be utilized.

Among the transition metals, osmium (hexagonal, $P6_3/mmc$) has the highest valence electron density (0.572 electrons $Å^{-3}$) and a very high (though somewhat contested) zero pressure bulk modulus between 395 and 462 GPa determined from in situ high-pressure diffraction experiments.[20–22,40] Recently, Pantea et al. measured the elastic constants of osmium single crystals using resonant ultrasound spectroscopy to obtain the bulk modulus. This method results in a much higher degree of accuracy and precision compared to conventional high-pressure diamond anvil cell (DAC) experiments and resulted in a bulk modulus of $(405 \pm 5)$ GPa for osmium, confirming its title as the least compressible metal.[23,41,42]

Our own experiments on osmium metal using a radial diffraction geometry in a DAC demonstrate that the metal has the ability to support remarkably high differential stress.[43] The use of radial diffraction geometry is an emerging technique that permits data collection on materials under non-hydrostatic stress. By directing the X-ray beam through the gasket rather than through the diamonds (Fig. 3), one can measure diffraction in both the maximum and minimum stress directions, thus determining the differential stress that each lattice plane can support. This enables one to gather information about the anisotropic nature of deformations in a material.[44] The differential stress also provides a lower bound estimate on the material's yield strength, that is, the stress at which point the material begins to deform plastically. At 25 GPa, osmium supports a maximum differential stress of 10 GPa for the (110) plane, the highest value for any measured metal.[43] Additionally, the (002) plane supports the least amount of stress before succumbing to plastic deformation, supporting the belief that such layered hexagonal materials are not as strong in the basal plane compared to the perpendicular (110) plane (a more involved discussion for hexagonal $ReB_2$ is presented below).

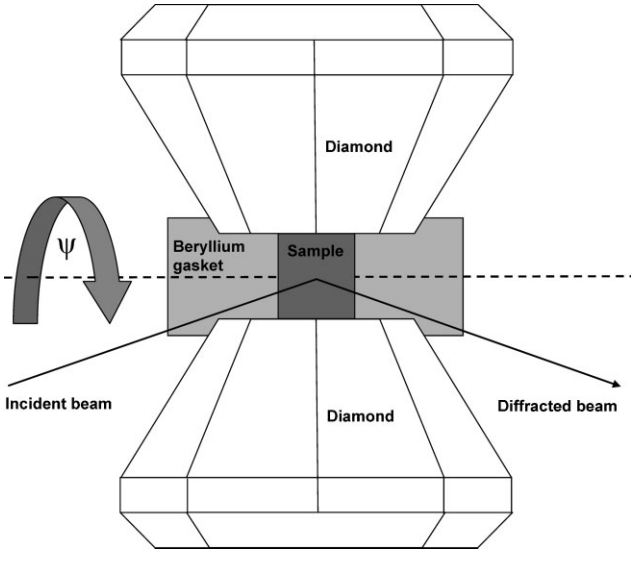


**Figure 3.** Radial diffraction geometry for high pressure experiments. The cell is rotated about the axis $\psi$, and data are collected through the gasket rather than through the diamonds as in conventional DAC experiments.

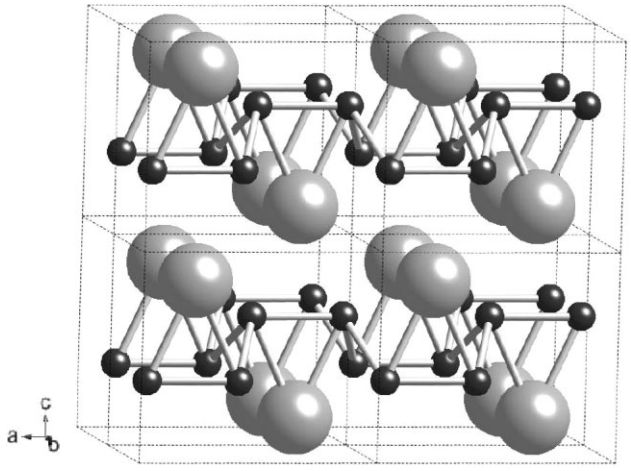


**Figure 4.** Multiple unit cells of $OsB_2$ (osmium—large atoms, boron—small atoms) stacked on top of one another. The B—B and Os—B covalent bonds are depicted which give rise to the relatively high hardness of $OsB_2$.

## 5. Osmium Diboride

Despite the exceedingly high bulk modulus and differential stress of osmium, its hardness is only 3.9 GPa.[45] This can be explained by the presence of non-directional metallic bonding in osmium. Applying our approach outlined above, we sought to introduce covalent bonds using boron to increase the hardness while maintaining the high bulk modulus of osmium. By employing a solid-state metathesis reaction containing a 2:3 mixture of $OsCl_3$:$MgB_2$ we were able to synthesize $OsB_2$ (orthorhombic, $Pmmn$) with a self-propagating reaction that was completed in under 1 second.[46] After washing away the $MgCl_2$ by-product salt, X-ray diffraction indicated the formation of $OsB_2$. $OsB_2$ was subsequently synthesized by two additional methods to produce either a fine powder for use in DAC experiments or a polycrystalline ingot for hardness measurements: a) heating a 1:5 molar ratio of Os:B at 1 000 °C for 3 days or b) reacting a 1:2.5 molar ratio of Os:B in an arc-melting apparatus under inert atmosphere. The unit cell for $OsB_2$, shown in Figure 4, has the following lattice parameters: $a = 4.684$ Å, $b = 2.872$ Å, $c = 4.096$ Å. It contains 2 osmium atoms located at the (a) site: (0.25, 0.25, 0.1535) and 4 boron atoms occupying the (f) site: (0.058, 0.25, 0.632).[47] The extended structure consists of two planes of osmium atoms separated by a puckered hexagonal layer of boron atoms in contrast to the $AlB_2$ structure which contains a planar array of boron atoms.[48]

Bulk modulus data for $OsB_2$ were collected at the Advanced Light Source, Lawrence Berkeley National Laboratory. A sample of $OsB_2$ was placed into a DAC and X-ray diffraction patterns where collected using the synchrotron radiation from ambient pressure to 32 GPa. From the diffraction data, the fractional volume change as a function of pressure was calculated. Fitting the

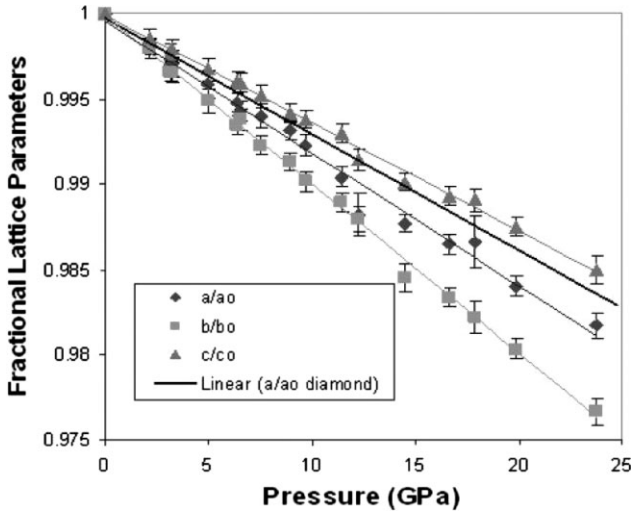


**Figure 5.** Comparison of the compressibility of the individual lattice parameters of $OsB_2$ with diamond. The *a* (◆), *b* (■), and *c* (▲) parameters in $OsB_2$ are fit with straight lines. Note that the *c*-axis in $OsB_2$ is less compressible than the analogous axis of diamond. Reproduced with permission from Ref. [46], copyright 2005 American Chemical Society.

pressure-volume data with a third order Birch–Murnaghan equation of state,

$$P = (3/2)B_0[(V/V_0)^{-7/3} - (V/V_0)^{-5/3}] \times \{1 - (3/4)(4 - B_0')[(V/V_0)^{-2/3} - 1]\} \quad (5)$$

the zero pressure bulk modulus, $B_0$, was calculated. The best fits were achieved with $B_0$ equal to 395 GPa and $B_0'$ (the derivative of the bulk modulus with respect to pressure) equal to 1.4. These

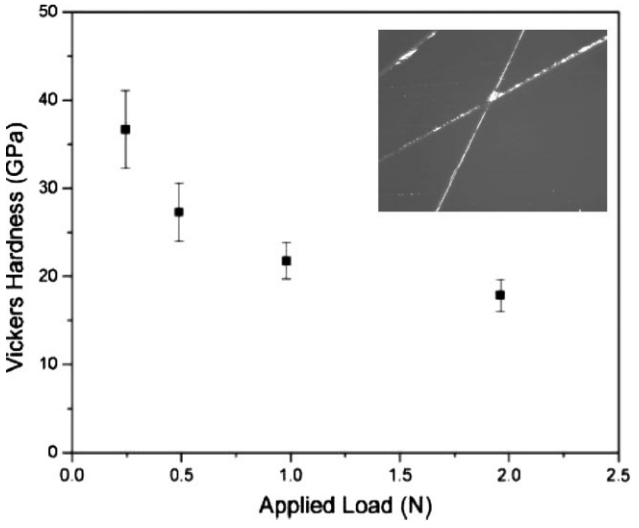


**Figure 6.** Vickers hardness of $OsB_2$, possessing a maximum hardness of 37 GPa. Inset: sapphire window scratched by $OsB_2$ powder viewed under 500 × magnification in an optical microscope. Adapted with permission from Ref. [50], copyright 2008 Materials Research Society.

numbers are exceptionally high, exceeding the bulk moduli of sapphire, silicon carbide, and cubic boron nitride.[49] Interestingly, the compressibility along the *c*-axis of $OsB_2$ even exceeds the linear compressibility of diamond (Fig. 5). Differences in the axial compressibilities arise from the anisotropy of the orthorhombic lattice. In the *a*–*b* plane, the osmium and boron atoms are offset from one another minimizing electrostatic repulsion under compression. Along the *c*-axis, however, the osmium and boron atoms are pushed into each other when compressed, maximizing the repulsive electrostatic forces, causing the higher observed incompressibility.[46]

Preliminary hardness values were determined using a qualitative scratch test based on the Mohs hardness scale that ranks materials on their ability to scratch another material. In this roughly logarithmic scale, talc is a 1 and diamond is a 10. $OsB_2$ readily scratches sapphire (a 9 on the Mohs scale), as shown in the inset to Figure 6, thus indicating that it possesses a hardness in the range of sapphire, ~15 GPa. More accurate hardness measurements were performed using micro- and nanoindentation methods. Microindentation tests were performed using a 4-sided Vickers diamond indenter with applied loads ranging from 0.25 N to 1.96 N. The residual indentations were measured and the hardness was calculated according to Equation 6:

$$H_V = 1.8544 \times \frac{P}{d^2} \quad (6)$$

where *P* is the applied load, *d* is the average diagonal length of the indent, and $H_V$ is the Vickers hardness. A Vickers hardness of 37 GPa was obtained for an applied load of 0.25 N and a value of 18 GPa was measured under a load of 1.96 N (Fig. 6). At forces greater than 2 N, the indentations tended to collapse, likely due to the brittleness of the material.[50] The large standard deviations depicted in Figure 6 are largely due to the anisotropy of the orthorhombic crystal structure and the polycrystalline nature of the arc-melted ingot. Electron backscattering diffraction coupled with hardness measurements reveal that in the (010) plane, the ⟨100⟩ direction is 54% harder than the ⟨001⟩ direction as indicated by the length of the indentation along the specific direction. This anisotropy arises from short covalent boron-boron bonds (1.80 Å) in the ⟨100⟩ direction, which prevent dislocation motion. These bonds are absent in the ⟨001⟩ direction because the interatomic distance between boron atoms is 4.10 Å.[50]

Nanoindentation tests were also performed using a 3-sided Berkovich diamond indenter. This method of hardness determination differs from the microindentation test by applying millinewtons of force rather than newtons, which is accompanied by indentation depths generally less than 1 000 nm, and by measuring indenter displacement during loading, rather than by imaging the static indentation after loading. The hardness is calculated according the method developed by Oliver and Pharr:[51]

$$H = \frac{P_{max}}{A} \quad (7)$$

where $P_{max}$ is the maximum applied load and *A* is the contact area of the diamond surface in the sample. Using a maximum load of 490 mN, a nanoindentation hardness of 21.6 GPa was obtained

which is within the range of values observed for the microindentation experiment. Additionally, a Young's modulus, also known as the elastic modulus, was obtained from the nanoindentation data using the theoretically calculated Poisson's ratio of 0.27.[52] A modulus of (410 ± 35) GPa was determined which is in good agreement with first-principles calculations that predicted a value of 426 GPa.[52] Determination of the elastic modulus by nanoindentation is based on the theory of contact mechanics for elastically *isotropic* materials.[51,53] Consequently, the indentation modulus calculated here is expected to differ from the Young's modulus because of the anisotropy inherent in the $OsB_2$ structure. However, the Young's modulus in the direction of the indentation will dominate the elastic response explaining why our result still yields a similar value to the predicted modulus.

Confirmation for the Vickers hardness was supplied by Hebbache et al. for arc-melted $OsB_2$. Under an equivalent load of 0.96 N, our material has a hardness of 22 GPa and their specimen has a hardness of 29 GPa. Whereas our data are representative of the average hardness for all crystallographic planes, their data were specifically collected for the (001) plane. Ab initio calculations performed by Hebbache indicate that the elastic constant, $C_{33}$, is significantly higher than either $C_{11}$ or $C_{22}$ suggesting that the hardness should be higher when measured in the (001) plane which is what is observed. Various first-principles theoretical studies have also been performed to elucidate the origin of osmium diboride's high hardness.[52,54–58] Electronic charge density contour plots and local density approximation density of states (DOS) calculations reveal that $OsB_2$ is metallic, but covalent bonding exists between B–B and Os–B leading to the high hardness, the latter due to strong overlap between the transition metal d states and the boron p states.[55,57]

The anisotropy of $OsB_2$ was further studied by density functional theory calculations to determine the ideal shear strength along specific crystallographic directions by Yang et al.[59] Their results reveal that in the (001) plane, the ideal shear strength along the ⟨010⟩ direction is 9.1 GPa, whereas along the ⟨100⟩ direction the ideal shear strength is nearly three times as large with a value of 26.9 GPa. The anisotropic behavior can be reconciled with a structural analysis. The high shear strength along the ⟨100⟩ direction is a direct result of the strong, covalently bonded B–Os–B triangles that resist shear along this direction. However, the low shear strength of 9.1 GPa results from sliding of the two adjacent osmium layers (Fig. 4) along ⟨010⟩ in which the B–Os–B triangles offer little resistance because they lie perpendicular (not parallel) to this direction of movement. The Vickers hardness for $OsB_2$ remains relatively high because the stronger resistance in the ⟨100⟩ direction dominates dislocation movement despite the low strength along the ⟨010⟩ direction.[59] Note that this analysis is not directly comparable to the hardness values in Ref. [50] although both reports illustrate the effect of anisotropy on the mechanical properties of $OsB_2$. Here, the directions ⟨100⟩ and ⟨010⟩ in the (001) plane are analyzed compared to the ⟨100⟩ and ⟨001⟩ directions in the (010) plane discussed by Chung et al. above. The analysis provided by Yang et al. illustrates the important role that anisotropy has on mechanical properties. The double osmium layer provides a definitive weak point in the lattice that should be avoided. Although this material is not superhard, it confirms the underlying theory behind designing hard materials. The covalent boron network serves to strengthen the osmium lattice while maintaining the metal's high incompressibility.

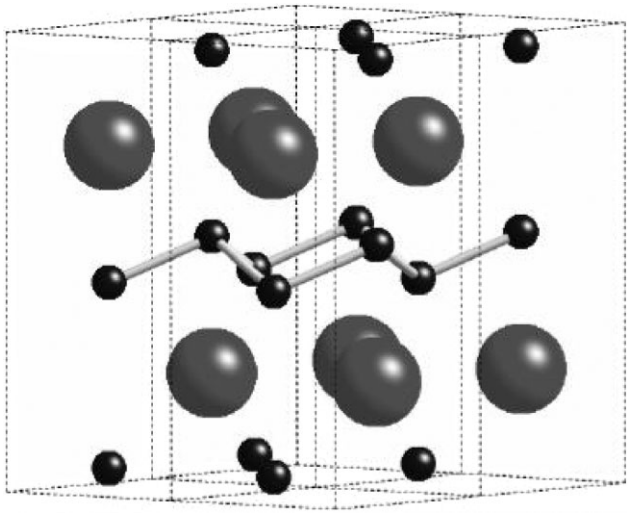

**Figure 7.** Multiple unit cells of $ReB_2$ illustrating the individual metal layers (large atoms) separated by a puckered boron network (small atoms).

## 6. Rhenium Diboride

In an effort to create potentially harder materials, we looked at utilizing rhenium instead of osmium. Rhenium diboride, originally synthesized in 1962, has the highest B:Re ratio among the known rhenium boride phases—$Re_3B$, $Re_7B_3$ and $ReB_2$—and is therefore the most likely candidate for improving on the mechanical properties of $OsB_2$.[60] Ideally, a rhenium compound that is more boron rich, such as the theoretical compound $ReB_4$, would be a preferred material using the rationale that a higher boron concentration results in a greater degree of covalent bonding, and thus a harder material. However, since no such compounds are known to exist, $ReB_2$ remains the best choice. Two additional points led us to believe that $ReB_2$ would be harder than $OsB_2$: i) $ReB_2$ does not contain any double metal layers that were shown to reduce the hardness for $OsB_2$ and ii) while $OsB_2$ produces a 10% expansion of the Os–Os bond distance upon incorporation of the boron atoms, inserting boron into the interstitial sites of rhenium produces only a 5% lattice expansion. This results in the shortest metal–metal bond length for any of the known transition metal diborides.[61] The crystal structure of $ReB_2$ (hexagonal, $P6_3/mmc$, $a = 2.900$ Å and $c = 7.478$ Å) is presented in Figure 7. It consists of alternating layers of hexagonally packed Re and puckered interconnected hexagonal rings of boron. The anisotropic nature of this compound, layered perpendicular to the *c*-axis along the (002) plane, should give rise to mechanical properties that are highly dependent on crystallographic orientation.

Rhenium diboride was synthesized by three methods: i) a solid-state metathesis reaction, ii) a combination of the elements by direct heating, and iii) arc-melting the elements.[62] $ReB_2$ powders synthesized directly from the elements under vacuum at 1 000 °C were used for high pressure diffraction studies, while ingots produced from arc-melting the elements under argon were used

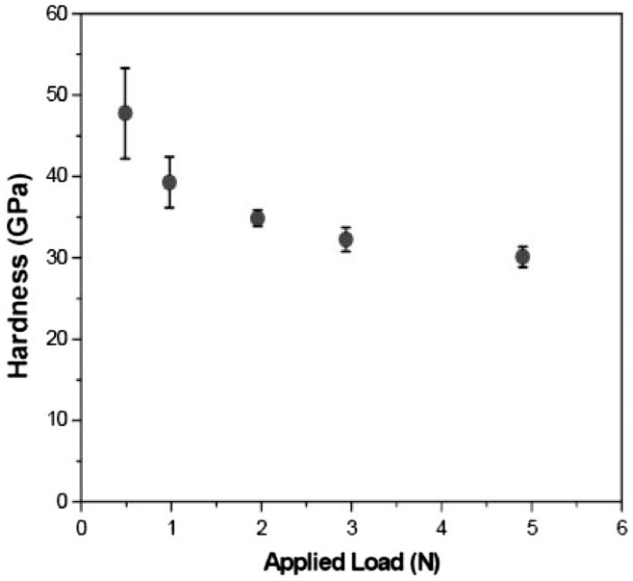


**Figure 8.** The Vickers hardness of $ReB_2$ is plotted as a function of applied load. The average hardness increases from 30 to 48 GPa as the applied load decreases from 4.9 to 0.49 N. Reproduced with permission from Ref. [62], copyright 2007 American Association for the Advancement of Science.

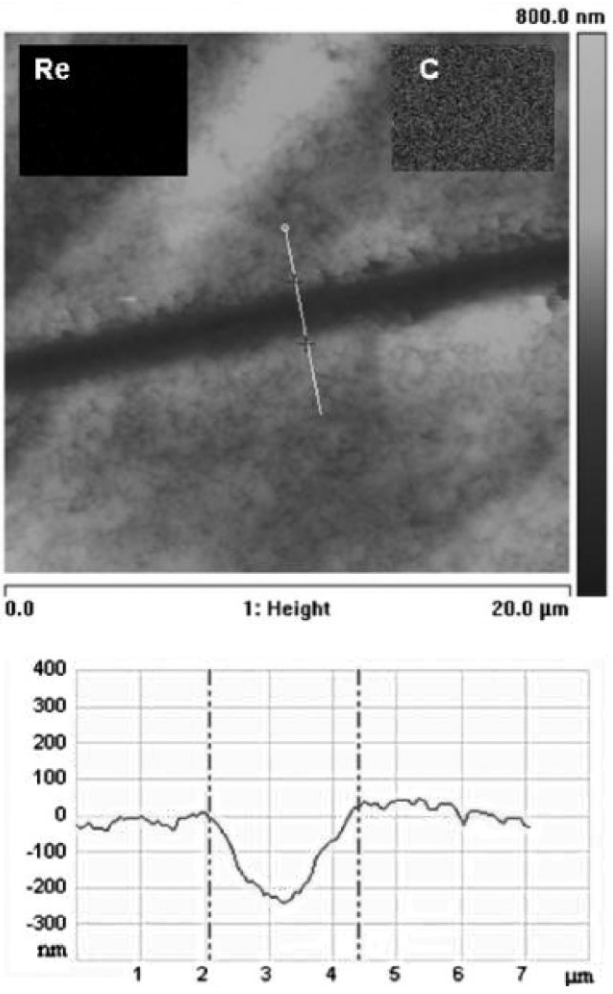


**Figure 9.** An AFM image (top) and depth profile scan (bottom) of a diamond surface scratched by $ReB_2$. The white line above corresponds to the depth profile below and the +'s indicate the dashed lines in the lower image. The scratch is approximate 230 nm deep and 2 µm wide. Elemental density maps (inset) indicate that carbon is uniformly distributed across the diamond (right) and that rhenium (left) has not been deposited on the diamond surface. Reproduced with permission from Ref. [64], copyright 2007 American Association for the Advancement of Science.

for hardness studies. A polished ingot of $ReB_2$ was tested with microindentation at various loads to determine the Vickers hardness. As the load was decreased from 4.9 to 0.49 N, the average hardness increased from $(30.1 \pm 1.3)$ to $(48.0 \pm 5.6)$ GPa (Fig. 8). A maximum hardness of 55.5 GPa was measured under a load of 0.49 N; this is comparable to cubic BN under an equivalent load.[63] With an average hardness of 48.0 GPa at low load, $ReB_2$ can be considered a superhard material ($H \geq 40$ GPa). The hardness of $ReB_2$ was qualitatively confirmed by a scratch test in which an arc-melted ingot was used to scratch the (100) plane of a natural diamond.

In response to our initial report on the mechanical properties of $ReB_2$, Dubrovinskaia et al. called into question the superhard nature of $ReB_2$ and the validity of the original diamond scratch.[12,62] Note that a scratch test is not a quantitative method for determining hardness, but rather a qualitative test indicating that $ReB_2$ has mechanical properties worthy of serious investigation. More conclusive evidence for the ability of $ReB_2$ to scratch diamond was provided via atomic force microscopy (AFM).[64] An ingot of $ReB_2$ was attached to a stylus and moved across a polished diamond surface using just the weight of the stylus to supply the force. Figure 9 shows an AFM image of the resulting scratch. The depth profile indicates that the scratch is 2-µm wide with a depth of approximately 230 nm. Energy dispersive X-ray (EDX) spectroscopic mapping (Fig. 9, inset) indicates that there is no detectable rhenium deposited on the surface of the diamond. To the best of our knowledge only four bulk materials have been previously reported to scratch diamond, all of which are regarded as superhard: c-BN, $B_6O$, fullerite, and diamond-like carbon.[8,10,31,33]

At low loads the hardness of many materials, including $ReB_2$, exhibit a strong dependence on load, increasing as the load decreases, known as the indentation size effect. For this reason, many people believe that hardness values calculated in this regime are meaningless. The asymptotic hardness of $ReB_2$, with a value of 30.1 GPa, lies well below the generally accepted value of 40 GPa for superhard materials. However, other materials, for example, transition metal borides and carbides, that have a comparable hardness to $ReB_2$ in the asymptotic region cannot scratch diamond (an assumption that is based upon the lack of any such reports in the literature). This suggests that the low-load data, which achieves its maximum average hardness of 48.0 GPa at 0.49 N, may provide an explanation for the ability of $ReB_2$ to scratch diamond. In addition, as stated earlier, the hexagonal structure of $ReB_2$ lends itself to mechanical anisotropy which may also serve to explain why $ReB_2$ can scratch diamond, despite an *average* hardness lower than that of other superhard materials. This topic is discussed in more detail below.

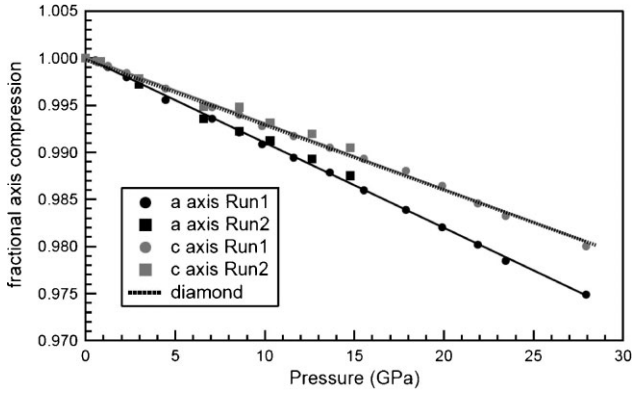


**Figure 10.** The fractional compression of $ReB_2$ separated into the *a*-axis and *c*-axis components to illustrate the anisotropic compressibility. The *a*-axis (dark symbols) is more compressible than the *c*-axis (light symbols). The *c*-axis of $ReB_2$ is as incompressible as the analogous axis of diamond (hashed line). Reproduced with permission from Ref. [62], copyright 2007 American Association for the Advancement of Science.

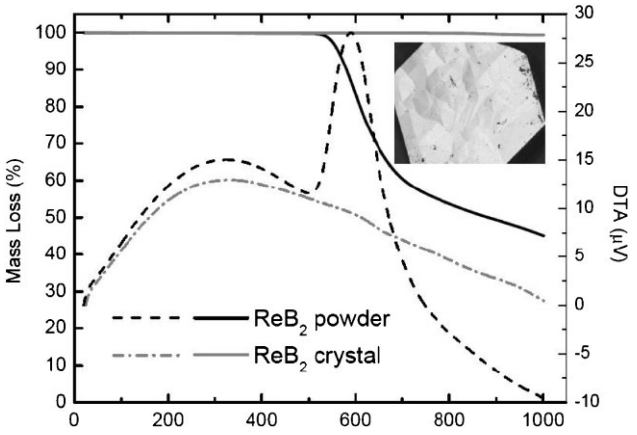


**Figure 11.** Thermogravimetric data for $ReB_2$ powder (black lines) and a $ReB_2$ crystal (grey lines). The crystal loses a negligible amount of mass (solid line) compared to the powder which undergoes rapid decomposition at 600 °C as indicated by the weight loss and large exothermic peak in the DTA curve (dashed lines). Inset: optical image of a $ReB_2$ crystal synthesized in an aluminum flux. Reprinted with permission from Ref. [76], copyright 2008 American Chemical Society.

The elastic properties of $ReB_2$ were studied via in situ high-pressure diffraction experiments.[62] In the first set of experiments, $ReB_2$ was compressed hydrostatically up to 30 GPa in a DAC and X-ray diffraction patterns were collected under pressure. Fitting the diffraction data with Equation 5 produced a bulk modulus for $ReB_2$ of 371 GPa for a $B_0'$ value of 0.84. $ReB_2$ has a valence electron density of 0.4774 $e^-$ $Å^{-3}$. Thus both the bulk modulus and the VED of $ReB_2$ are slightly lower than the values for $OsB_2$ (VED = 0.5102 $e^-$ $Å^{-3}$), in good agreement with our understanding of the correlation between valence electron density and incompressibility.

Analysis of the fractional volume change with respect to pressure again revealed anisotropy in the compressibility of the two different lattice directions of $ReB_2$, with the *c*-axis substantially less compressible than the *a*-axis (Fig. 10).[62] Here the *c*-axis value is comparable to the analogous linear compressibility of diamond. As with $OsB_2$, this anisotropy likely results from greater electron density, and therefore greater electronic repulsions, along the *c*-axis.

$ReB_2$ was also intentionally subjected to non-hydrostatic pressure in radial diffraction experiments to determine how different crystallographic planes in the material support different amounts of stress before plastic deformation occurs. Data were collected from 0 to 30.1 GPa with $ReB_2$ supporting a lattice averaged differential stress of 6.4 to 12.9 GPa, the highest values measured for any material at these pressures.[65–67] The (004) plane, which lies parallel to the layers of Re and B, supports the least amount of stress due to the ability of the layers to slide across one another in this plane. The (110) plane, which lies orthogonal to Re and B layers, is the stiffest plane and therefore exhibits the greatest ability to support differential stress.

This same anisotropy was directly observed in hardness measurements, using electron backscattering diffraction (EBSD) to determine the crystallographic orientation of each grain that was indented. The results confirm that for the hardness measurements, indentations parallel to (002) yield the lowest average hardness. In contrast, indentations along directions that contain a larger component parallel to the *c*-axis, that is, perpendicular to (002), result in measurements with an average hardness that is 15% higher. For example, under a load of 4.9 N, indentations parallel to (002) yield the lowest average hardness with a value of 27 GPa. Conversely, indentations approaching the orthogonal plane possess an average hardness of 31 GPa. This difference, which was also observed in radial diffraction experiments illustrates the effect of anisotropy on the mechanical properties and highlights the need for growing single crystals in order to properly characterize this material.

An extended experimental study of the physical properties of $ReB_2$ single crystals had not yet been performed despite reports of $ReB_2$ crystals synthesized by both zone melting and optical floating zone methods.[68,69] Additionally, several theoretical studies have reported on the electrical, thermal, and rheological properties of $ReB_2$ in an effort to better understand this material's unique combination of properties.[54,70–75] The use of single crystals is clearly necessary to experimentally verify these results because many of the properties are altered by grain boundaries in polycrystalline samples. Thus, we recently reported on the first synthesis and characterization of $ReB_2$ crystals grown by a flux technique.[76]

Aluminum was chosen as a suitable flux for crystal growth based on prior experiments synthesizing various other transition metal borides and the high solubility of both boron and rhenium in aluminum.[77–85] Crystals were grown from the initial molar composition Re/B/Al equal to 1:2:50 in an alumina crucible under an inert gas by slow cooling the melt from 1 400 °C to 700 °C at a rate of 5 °C $h^{-1}$.[76] The resulting crystals were separated from the solidified melt using concentrated NaOH. The crystals grew to a maximum size of 3 mm in diameter and had well defined hexagonal symmetry (Fig. 11, inset). X-ray diffraction confirmed that the crystals grow oriented with respect to the (002) plane in accordance with crystals synthesized in an optical floating zone furnace.[69] Chemical analysis (ICP-AES) indicated that the crystals are slightly boron deficient and contain small amounts of

aluminum flux incorporated into the lattice, giving a true composition of $ReAl_{0.011}B_{1.85}$. This is to be expected when using the flux method and both aluminum inclusions and defective boron layers have been reported previously for flux grown metal diborides.[82,84,85]

Microindentation performed on the (002) and perpendicular (*hk*0) planes confirmed the mechanical anisotropy of $ReB_2$. The highest low-load hardness had an average value of 40.5 GPa reported for the (002) plane; this is about 6% higher than the hardness measured for the (*hk*0) plane. Nanoindentation also confirmed the higher hardness of the (002) plane with a value of 36.4 GPa which is approximately 7% higher than the perpendicular plane with a nano-hardness value of only 34.0 GPa. The difference in hardness for both planes is in good agreement with the Vickers microindentation anisotropy and the EBSD data collected for arc-melted $ReB_2$; however the Vickers hardness data are lower than the values reported for arc-melted $ReB_2$ by about 15%.[62] This decrease in hardness for the single crystal can be attributed to the boron-deficient network. A 7.25% reduction in boron concentration (1.85/2.00) would reduce the degree of covalent bonding and thus lower the overall hardness of the crystal. Additionally, crystals generally have lower hardness compared to equivalent polycrystalline materials because of the lack of grain boundaries which serve to inhibit crack propagation and increase hardness.[86,87]

Nanoindentation was also used to calculate the elastic modulus for the two perpendicular directions of the flux-grown crystals. An indentation modulus of 675 GPa was reported for the basal plane; with a corresponding value for the (*hk*0) plane of 510 GPa. Although the elastic moduli anisotropy is consistent with the hardness measurements indicating a greater resistance to plastic and elastic deformation along the *c*-axis, the observed indentation moduli differ by about 25% compared to only 7% for the nano-hardness data. This discrepancy can be reconciled by careful manipulation of the elastic constants as calculated by Hao et al.[88] according to Equations 8 and 9:

$$k_c/k_a = (C_{11} + C_{12} - 2C_{13})/(C_{33} - C_{13}) \quad (8)$$

$$A = 2C_{44}/(C_{11} - C_{12}) \quad (9)$$

where $k_c/k_a$ measures the degree of compressional anisotropy for the *c* and *a* directions, and *A* indicates the degree of shear anisotropy. $ReB_2$ has values of $k_c/k_a = 0.56$ and $A = 1.06$ (an isotropic material would have a value of 1 for both terms).[89] These numbers indicate that elastic compression is more anisotropic than shear. Since hardness is more strongly correlated with shear strength than compressive strength it is expected that hardness should be more isotropic than the elastic modulus, as observed from our measurements on the flux crystals.

One of the benefits of single crystals is the ability to perform electrical resistivity measurements that are not hindered by the presence of grain boundaries. The in-plane resistivity along the (002) plane was measured from 12.5 K up to 300 K using a standard four-point probe configuration.[76] $ReB_2$ exhibits metallic conductivity with a room temperature resistivity of $\rho_{ab}(300\ K) = 40.7\ \mu\Omega$ cm and a residual resistivity ratio of 13. This result is consistent with theoretical calculations that predicted a nonzero density of states at the Fermi level due to overlap of the 5 d orbitals of Re with the 2p orbitals of B.[88] $ReB_2$ is the only bulk superhard material reported so far to exhibit metallic conductivity. The majority of superhard materials are insulators because of the strong covalent bonds that necessitate a large band gap from the filling of the bonding orbitals, while leaving the antibonding orbitals empty (e.g., diamond has a band gap $E_g = 5.4$ eV[17]).

A major difference between the flux crystal and polycrystalline samples was elucidated by thermogravimetric analysis (Fig. 11).[76] Upon heating in dry air, $ReB_2$ powder loses a significant portion of its mass at 600 °C. The mass loss continues up to 1 000 °C, totaling over 50% of the original sample mass. Because boron comprises only 10% of the mass of $ReB_2$, the change in weight is attributed to the loss of rhenium by the formation of volatile $ReO_3$. $ReB_2$ crystals, in contrast, remain stable until at least 800 °C, at which point the crystals lose only a negligible percentage of their mass. The enhanced stability of the $ReB_2$ crystals is likely due to the leaching of boron from the lattice which reacts with oxygen to form a protective surface coating of $B_2O_3$ that in turn lowers the rate at which any further oxidation might occur. The thermal response of $ReB_2$ contrasts with the behavior of other borides that form stable transition metal oxides upon heating, resulting in weight gains ranging from a few percent (e.g., $WB_2$) to an excess of 20% (e.g., $TaB_2$).[81,82] The resistance of $ReB_2$ crystals to thermal degradation and their ability to freely conduct electricity could pave the way for the development of superhard coatings with promising technical capabilities for use in the defense and aerospace industries.

## 7. Shear Modulus of $MB_2$

In the search for new materials, various indicators have been used to predict superhard materials. As discussed above, a high hardness requires limiting the creation and mobility of dislocations which is largely governed by the resolved shear stress of the material. However, this property is difficult to measure and so consequently the shear modulus is often used for predicting hard materials. As a validation of this practice, the hardness of three diborides was measured via nanoindentation methods and the correlation with the isotropically derived bulk modulus and shear modulus was determined.[19]

The diborides were synthesized by arc-melting the elements Ru, Os, and Re with amorphous boron as described in Ref. [62] to form $RuB_2$, $OsB_2$, and $ReB_2$, respectively. Hardness values were determined using nanoindentation with a maximum applied load of 720 mN on the polished ingots. The average measured hardness was $(19.2 \pm 2.1)$, $(21.6 \pm 3.0)$, and $(37.0 \pm 1.2)$ GPa for $RuB_2$, $OsB_2$, and $ReB_2$, respectively.[19] $ReB_2$ is significantly harder that both the ruthenium and osmium borides in agreement with our previous results. The difference in hardness between $RuB_2$ and $OsB_2$, which should be isolectronic, is attributed to relativistic effects of osmium resulting in greater orbital overlap and consequently stronger covalent Os−B bonds in $OsB_2$ compared to $RuB_2$.[90] The discrepancy between the nanoindentation values and Vickers hardness previously reported is likely due to the differences in the indenter shape, depth of penetration, and

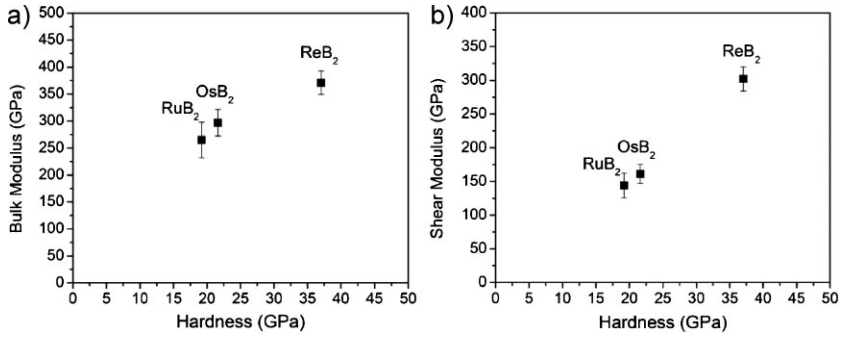


**Figure 12.** Hardness plotted as a function of bulk modulus (left) and shear modulus (right) illustrating the better correlation between hardness and shear modulus. Reprinted with permission from Ref. [19], copyright 2008 American Institute of Physics.

method of measurement (Vickers hardness measures the residual indentation, which overlooks the material's elastic response).[19,50]

Nanoindentation experiments enabled the determination of the Young's moduli for these compounds which were then used to calculate the corresponding bulk and shear moduli based on a homogeneous isotropic model according to Equations 10 and 11:[91]

$$\frac{1}{E} = \frac{1}{3G} + \frac{1}{9B} \tag{10}$$

$$\nu = \frac{1}{2}\left[1 - \frac{3G}{3K+G}\right] \tag{11}$$

The resulting values were found to agree reasonably well with both the experimental and first principles calculations for the elastic moduli.[19,46,52,55–57,62,88] The hardness as a function of bulk modulus and shear modulus are plotted in Figure 12. The data for bulk modulus are clearly nonlinear with respect to hardness, while the data for the shear modulus follow a linear path. This is due to the insensitivity of bulk modulus to the details of bonding, while the shear modulus is much more dependent on both bond strength and directionality. For example, the double metal atom layers present in $OsB_2$ and $RuB_2$ produce some directionless bonds that reduce both the hardness and the shear modulus but have no negative effect on the bulk modulus. The data, therefore, confirm that these Os−Os interactions have no negative effect on the bulk modulus, however, the data confirm the hypothesis that bulk modulus is a necessary but insufficient condition for predicting superhard materials.

## 8. Powder Compacts of Rhenium Diboride

The superhard nature of $ReB_2$ has continually been under scrutiny due to the low values reported for hardness at high load.[12,92] Recently, Qin et al. synthesized $ReB_2$ under high pressure and determined the mechanical properties via conventional high-load Vickers indentation techniques and ultrasound experiments. $ReB_2$ compacts were obtained by reacting elemental rhenium with amorphous boron with a molar ratio of 1:2.5 under 5 GPa of pressure at 1 600 °C for 60 min.[92] Vickers hardness measurements revealed a hardness of only (18.4 ± 1) GPa under a load of 4.9 N and (16.9 ± 0.6) GPa under the maximum tested load of 49 N. The obtained hardness at 4.9 N is substantially lower than the value of 30.1 GPa reported for arc-melted $ReB_2$.[62] This is likely due to the addition of 0.5 moles of excess amorphous boron into the compact. Although the additional boron produces a phase pure product according to powder X-ray diffraction measurements, the excess boron distributed through the compact drastically reduces the hardness of the material. We have observed this effect in our own research with powder compacts of rhenium diboride densified by spark plasma sintering at 1 400 °C under 50 MPa of pressure. The specimen contained an additional 10% (0.2 moles) of boron and possessed a Vickers hardness of only (17.5 ± 2.6) GPa under an applied load of 4.9 N.

To determine the bulk elastic properties of the compacts Qin et al. performed sound velocity measurements using a pulse-echo method. An ultrasonic pulse generated from a quartz crystal was sent through the sample and the wave velocity was determined by dividing the distance traveled by the time necessary to complete the journey. Using this method, they calculated values for the Young's modulus, shear modulus, bulk modulus, and Poisson's ratio of 382 GPa, 169 GPa, 173 GPa, and 0.0966, respectively. These values are compared with the values for arc-melted $ReB_2$ from our previous papers in Table 1.[19,62] All three elastic constants are significantly lower (~50%) for the $ReB_2$ compact than for the arc-melted sample. Once again, this can be attributed to the presence of amorphous boron in the compact that likely results in lower sound velocities and consequently lower elastic constants. Additionally, Qin et al. did not take into consideration the anisotropic nature of $ReB_2$. They used the elastic stiffness relationships for isotropic solids, which is clearly not valid for $ReB_2$. The anisotropic factor for the elastic modulus of flux-grown $ReB_2$ discussed above was determined to be 0.56. Thus, the use of isotropic relationships will result in over-simplification and an underestimation of the elastic constants.

The above discussion illustrates the discrepancies that can arise between different experimental techniques. The amorphous boron present in the powder compacts has a detrimental effect on bulk modulus sound wave experiments, yet does not affect the bulk modulus calculated by high pressure diffraction because in the high pressure experiment, compression is measured at the atomic scale using X-ray diffraction, rather than on the whole composite material. High pressure diffraction experiments,

**Table 1.** The elastic constants of arc-melted $ReB_2$ and densified powder compacts of $ReB_2$ determined by various methods.

| $ReB_2$ morphology | *E* (GPa) | *G* (GPa) | *B* (GPa) | $H_v$[a] (GPa) |
|---|---|---|---|---|
| Powder compact of $ReB_2$ + 0.5B | 382[b] | 169[b] | 173[b] | 18.4[b] |
| Arc-melted pellet of $ReB_2$ | 712[c] | 302[c] | 371[d] | 30.1[d] |

[a] Hardness values are reported under an applied load of 4.9 N. [b] Ref. [92]. [c] Ref. [19]. [d] Ref. [62].

however, can suffer from non-hydrostatic conditions in the sample chamber which can artificially inflate the obtained value for bulk modulus. Thus, it would be helpful to corroborate the elastic constants obtained for $ReB_2$ by conventional techniques with an alternative method. With the help of collaborators at that University of Nevada, Las Vegas, we recently determined the shear modulus of a densified powder compact of $ReB_2$ by surface Brillouin scattering.[93] The $ReB_2$ compact is only 86% dense and possesses a shear modulus of 173 GPa, confirming the belief that amorphous boron has a detrimental effect on the mechanical properties. Additional experiments are underway to determine the elastic constants via resonant ultrasound spectroscopy of arc-melted, single crystals of $ReB_2$ that have densities close to the theoretical value.[41,42,94] Preliminary results indicate that single crystalline $ReB_2$ possesses a shear modulus of 273 GPa and a bulk modulus of 382 GPa, in excellent agreement with our previous results.

## 9. The Future of Superhard Metal Borides

The previous sections present an in-depth analysis of the synthesis and characterization of various transition metal diborides in the search for new ultra-incompressible superhard materials. The goal throughout this project has been to create these materials without the application of high pressure. Rhenium diboride has satisfied this criterion as a polycrystalline ingot[62] and as a single crystal[76] with hardness values greater than 40 GPa under low loads. The rationale of adding covalent bonding to dense transition metals has thus effectively opened up a new field of research that has resulted in over 20 publications worldwide during just the past two years. Here we present a few new results both from our group and the larger scientific community that should lead to enhanced mechanical properties of transition metal borides in addition to spurring efforts towards creating new superhard materials without the need for high pressure.

Many applications for superhard materials necessitate that the material be applied as a thin film or coating. This is clearly advantageous for a material containing a relatively expensive platinum group metal where reduced metal consumption will improve the cost effectiveness. In order for a coating to be potentially useful it must possess a combination of mechanical and physical properties: chemical stability, thermal stability, oxidative resistance, good adhesion to the substrate, high fracture toughness and high hardness.[95] Such superhard coatings can be used for cutting tools and drill bits, leading to increased hardness, reduced wear, and ultimately longer tool lifetimes. Additionally, many coatings exhibit low friction coefficients which reduce shear forces between two sliding surfaces and increase a tool's durability.[96] Diamond, sapphire, various carbides and nitrides (e.g., TiC, TiN, c-$Zr_3N_4$), and recently c-BN have all been deposited as coatings onto high speed cutting tools because of their improved mechanical properties compared to the substrate to which they are applied.[97–99] Moreover, under certain conditions many materials exhibit an increase in hardness when synthesized as a film compared to the bulk material. This enhancement involves a complex interaction of decreasing grain size, densification of grain boundaries, formation of point defects, and compressive stress resulting from deposition, all of which may serve to limit dislocation mobility.[100,101] $ReB_2$, as an intrinsic superhard material, is therefore an excellent candidate for forming coatings that enhance mechanical properties.

Latini et al. recently obtained the first films of $ReB_2$ and found them to be superhard.[102] An initial target was synthesized by melting rhenium and boron powder to form $ReB_2$. Pulsed laser deposition was used to evaporate the target and collect the material on a $SiO_2$ substrate. X-ray diffraction indicated a phase pure $ReB_2$ film with a preferred orientation along (002). Scanning electron microscopy revealed an average crystallite size of 100 nm and a film thickness of $(0.30 \pm 0.5)$ μm. An area law-of-mixtures approach was used to determine the hardness of the film which has previously been experimentally demonstrated to be in good agreement with theoretical models.[103–106] The intrinsic hardness for the deposited $ReB_2$ film was $(52 \pm 6)$ GPa, exceeding the hardness of any other metal diboride coating and in good agreement with the bulk samples prepared by arc-melting.[62,102]

Pulsed laser deposition has also been used to prepare superhard ruthenium boride films.[107] Starting from a pure $RuB_2$ target, a biphasic ruthenium boride film composed of $RuB_2$ and $Ru_2B_3$ was deposited on an $SiO_2$ substrate with an average thickness of $(0.7 \pm 0.1)$ μm. The film is composed of approximately 35% $RuB_2$ and 65% $Ru_2B_3$ by volume with grain sizes in the range of 2 nm – 250 nm, as determined by XRD and SEM analysis. The Vickers hardness of the $RuB_2$ target used for the deposition varied from 10.9 GPa under a load of 9.8 N to a maximum value of 17.0 GPa under a load of 0.49 N. These values are in reasonable agreement with our results on arc-melted $RuB_2$ which possesses a Vickers hardness of 20.6 GPa under a load of 0.49 N.[90] Because the deposited film contained $Ru_2B_3$, in addition to $RuB_2$, however, the hardness of a $Ru_2B_3$ target was also measured and found to be similar to the values for $RuB_2$. The intrinsic hardness for the ruthenium boride film was $(49 \pm 6)$ GPa, which is significantly higher than either of the constituent bulk materials. The enhanced hardness of this material was attributed to the nanocrystallinity of the film which serves to pin dislocations through grain boundaries and suggests that further superhard materials could by synthesized by adjusting the morphology of the bulk compounds to create nanostructured materials.[108]

The concept of introducing light p-block elements into transition metal lattices has been shown to be an effective method for increasing the hardness of materials with the formation of metal diborides.[2,3,19,50,62,109] The addition of two boron atoms per metal atom induces covalent bonding that strengthens the lattice. One would, therefore, expect that higher concentrations of boron would continue to increase the hardness of the material. Unfortunately, most transition metal-boron compounds are metal rich with low boron to metal ratios. Tungsten, however, can form $WB_4$ which contains twice as many boron atoms as the diborides discussed throughout this article. This has two advantages: i) the lower metal content reduces the overall cost of production since amorphous boron is relatively inexpensive compared to the cost of most transition metals and ii) the higher boron content lowers the density of the compound compared to the analogous diboride which lowers the weight of the material–a benefit for many potential applications.

Tungsten tetraboride, $WB_4$ (hexagonal, $P6_3/mmc$), was originally discussed by Brazhkin et al. and its potential as a superhard

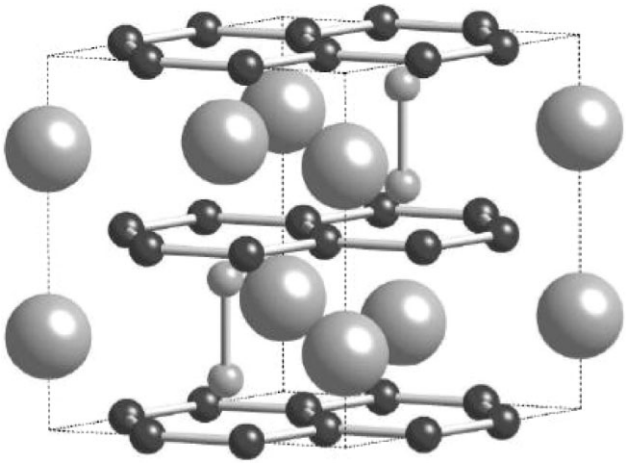

**Figure 13.** The crystal structure of $WB_4$. The boron atoms (small atoms) form a hexagonal network in addition to covalent dimers that result in a 3-dimensional network. The tungsten atoms (large atoms) form hexagonal layers in between the boron sheets.

material was emphasized in our *Science* perspective.[2,4] It has a VED of 0.485 $e^-$ $Å^{-1}$ which is comparable to the VED of $ReB_2$ (0.477 $e^-$ $Å^{-1}$), suggesting that this compound might be ultra-incompressible. Gu et al. recently synthesized $WB_4$ by arc-melting and measured the mechanical properties.[110] A bulk modulus of 200 GPa was obtained by X-ray diffraction in a DAC. This value is surprisingly low, considering the high VED of $WB_4$ and the high bulk modulus of elemental tungsten, 308 GPa.[4] The electron localization function was calculated for $WB_4$, indicating that the boron framework dominates the compressibility response, while the W atoms sit in the voids in the lattice.[110] Thus, the compressibility of $WB_4$ should be comparable to elemental boron with a bulk modulus of 185 GPa, which is what is observed.[111]

The Vickers hardness of $WB_4$ was reported to be quite high with a value of $(46.2 \pm 1.2)$ GPa under an applied load of 0.49 N and a load-independent hardness of $(31.8 \pm 1.2)$ GPa, which is nearly equivalent to the hardness of arc-melted $ReB_2$ under a load of 4.9 N ($(30.1 \pm 1.3)$ GPa). The high hardness of $WB_4$ is attributed to its unique boron network (Fig. 13). $WB_4$ consists of alternating layers of hexagonal networks of boron (not puckered as in $ReB_2$) and hexagonal layers of tungsten atoms.[112] In between the boron layers are $B_2$ dimers aligned along the *c*-axis. First principle calculations reveal a finite density of states at the Fermi level, indicating that $WB_4$ is metallic.[113] Furthermore, it was discovered that there is only weak covalent bonding between tungsten and boron. The high hardness of the material is therefore due to the covalent bonds in the layered boron network and extremely strong bonds in the $B_2$ dimer. Without the $B_2$ dimers, the covalent bonds would be restricted to the *a*–*b* plane and $WB_4$ would behave like a layered compound similar to graphite. However, the presence of the B−B bonds along the *c*-axis results in a three-dimensional covalent network that resists plastic deformation.[113] $Mo_{0.8}B_3$ (hexagonal $P6_3/mmc$) has a similar structure to $WB_4$ except that it is missing the $B_2$ dimers.[114] It has an equally high VED of 0.481 $e^-$ $Å^{-1}$ and is predicted to be ultra-incompressible. The absence of the dimers, however, should result in lower hardness values compared to $WB_4$. The synthesis and subsequent testing of the mechanical properties of $Mo_{0.8}B_3$ would be beneficial to elucidate the role of the dimers in $WB_4$.

A discussion of the details of bonding in similar metal borides leads one to reconsider the possible origin for the superhard nature of $ReB_2$ based on its bonding. Although many other borides have hexagonal symmetry, the majority of the transition metal borides crystallize in the $AlB_2$ structure. This structure consists of alternating hexagonal nets of metal atoms and planar hexagonal nets of boron atoms.[115] In contrast, $ReB_2$ contains puckered hexagonal rings of boron atoms between the hexagonal array of rhenium atoms. The resulting structure contains shorter M−B bonds than the corresponding $AlB_2$ structure. It is likely that these short bonds contribute to the material's impressive mechanical properties.

Just as c-BN was synthesized in order to mimic the crystal structure of diamond,[31] new transition metal borides can now be synthesized with the $ReB_2$ structure in the search for new superhard materials. This approach has two advantages. First, the underlying methodology used to create incompressible, superhard materials will continue to apply for these systems – dense metals with high valence electron densities will once again be combined with boron to introduce strong covalent bonds.[2,3,46] Second, by reducing the amount of rhenium in these materials, the cost may be lowered, thus improving the attractiveness for potential applications.

No additional binary borides have been reported with the $ReB_2$ structure except for $TcB_2$, and no ternary phases were found to exist containing Re, B, and a platinum group metal.[116] However, seven compounds have been reported to crystallize with the $ReB_2$ structure: $M^{VI}_{0.3}M^{VIII}_{0.7}B_2$ ($M^{VI}$ = Mo, W, $M^{VIII}$ = Ru, Os), $V_{0.4}Os_{0.6}B_2$, $Mo_{0.6}Ir_{0.4}B_2$, and $W_{0.56}Ir_{0.44}B_2$.[116–118] All of the $ReB_2$-type structures contain an element to the left of rhenium and an element to the right, thereby maintaining an electron/atom ratio of 4.3–4.4 ($e^-$ per atom for $ReB_2 = 4.33$). This is advantageous if we are to effectively mimic the properties of $ReB_2$ without using rhenium. It is important to note that ruthenium and osmium are the least compressible elements in their respective rows of the periodic table and so we predict that mixed metal borides like those described above will also be ultra-incompressible.[3]

Several of the compounds with the $ReB_2$ structure have not yet been isolated in their pure forms. The structures were determined from X-ray diffraction patterns containing multiple phases. Synthesizing these compounds is therefore not a trivial task. Preliminary experiments on $W_{0.3}Ru_{0.7}B_2$ indicate that although the compound exists in arc-melted pellets, a phase pure sample cannot be obtained through this route. In this case, flux growth could provide a reaction pathway to a phase pure product since incongruently melting compounds as well as many transition metal diborides have been synthesized in this manner by careful control of the reactant ratios, temperature profiles, and dwell times.[77,82,84,85] Further research into the synthesis and mechanical characterization of these materials will provide valuable insight into the superhard nature of the $ReB_2$ structure-type.

The future of this relatively new field of research is still rife with possibilities—higher borides such as $WB_4$ have shown the importance of increasing covalent bonding. The introduction of light metals into a boron network (e.g., $Li_2B_6$, and $BeB_6$) should also result in highly covalent short bonds and deserves investigation.

Similarly thin films have only just begun to be synthesized for this new class of ultra-incompressible superhard materials and should further increase the hardness. Densification of nanocrystalline powders also deserves exploration for potentially enhancing the mechanical properties of these metal borides.

## Acknowledgements

The authors would like to thank the National Science Foundation Grant DMR-0805357 for continued support of this research.

Received: July 13, 2009
Published online: October 20, 2009

[1] V. Brazhkin, N. Dubrovinskaia, M. Nicol, N. Novikov, R. Riedel, V. Solozhenko, Y. Zhao, *Nat. Mater.* **2004**, *3*, 576.
[2] R. B. Kaner, J. J. Gilman, S. H. Tolbert, *Science* **2005**, *308*, 1268.
[3] J. J. Gilman, R. W. Cumberland, R. B. Kaner, *Int. J. Refract. Met. Hard Mater.* **2006**, *24*, 1.
[4] V. V. Brazhkin, A. G. Lyapin, R. J. Hemley, *Philos. Mag. A* **2001**, *82*, 231.
[5] V. V. Brazhkin, *High Pressure Res.* **2007**, *27*, 333.
[6] S. Veprek, M. J. G. Veprek-Heijman, *Surf. Coat. Technol.* **2008**, *202*, 5063.
[7] S. Veprek, A. S. Argon, *J. Vac. Sci. Technol. B* **2002**, *20*, 650.
[8] N. Dubrovinskaia, L. Dubrovinsky, W. Crichton, F. Langenhorst, A. Richter, *Appl. Phys. Lett.* **2005**, *87*, 831061.
[9] N. Dubrovinskaia, V. L. Solozhenko, N. Miyajima, V. Dmitriev, O. O. Kurakevych, L. Dubrovinsky, *Appl. Phys. Lett.* **2007**, *90*, 1019121.
[10] V. Blank, M. Popov, G. Pivovarov, N. Lvova, K. Gogolinsky, V. Reshetov, *Diamond Relat. Mater.* **1998**, *7*, 427.
[11] V. D. Blank, S. G. Buga, G. A. Dubitsky, K. V. Gogolinsky, V. M. Prokhorov, N. R. Serebryanaya, V. A. Popov, in *Molecular Building Blocks for Nanotechcnology – From Diamondoids to Nanoscale Materials and Applications*, (Ed.: G. A. Mansoori), Springer Science, New York **2007**.
[12] N. Dubrovinskaia, L. Dubrovinsky, V. L. Solozhenko, *Science* **2007**, *318*, 1550c.
[13] J. J. Gilman, *Electronic Basis of the Strength of Materials*, Cambridge University Press, Cambridge **2003**.
[14] J. Haines, J. M. Léger, G. Bocquillon, *Annu. Rev. Mater. Res.* **2001**, *31*, 1.
[15] B. R. Sahu, L. Kleinman, *Phys. Rev. B* **2005**, *72*.
[16] C. H. Li, P. Wu, *Chem. Mater.* **2001**, *13*, 4642.
[17] *CRC Handbook of Chemistry and Physics* (Ed: D. R. Lide), CRC **2008**.
[18] D. M. Teter, *MRS Bull.* **1998**, *23*, 22.
[19] H.-Y. Chung, M. B. Weinberger, J.-M. Yang, S. H. Tolbert, R. B. Kaner, *Appl. Phys. Lett.* **2008**, *92* 261904.
[20] T. Kenichi, *Phys. Rev. B* **2004**, *70*, 012101/1.
[21] F. Occelli, L. Farber Daniel, J. Badro, M. Aracne Chantel, M. Teter David, M. Hanfland, B. Canny, B. Couzinet, *Phys. Rev. Lett.* **2004**, *93*, 095502.
[22] H. Cynn, J. E. Klepeis, C.-S. Yoo, D. A. Young, *Phys. Rev. Lett.* **2002**, *88*, 135701/1.
[23] C. Pantea, I. Mihut, H. Ledbetter, J. B. Betts, Y. Zhao, L. L. Daemen, H. Cynn, A. Migliori, *Acta Mater.* **2009**, *57*, 544.
[24] J. M. Leger, P. Djemia, F. Ganot, J. Haines, A. S. Pereira, J. A. H. da Jornada, *Appl. Phys. Lett.* **2001**, *79*, 2169.
[25] W. A. Harrison, *Electronic Structure and the Properties of Solids*, Freeman, San Francisco **1980**.
[26] M. L. Cohen, *Science* **1993**, *261*, 307.
[27] I. V. Aleksandrov, A. F. Goncharov, A. N. Zisman, S. M. Stishov, *Zh. Eksp. Teor. Fiz.* **1987**, *93*, 680.
[28] A. Migliori, H. Ledbetter, R. G. Leisure, C. Pantea, J. B. Betts, *J. Appl. Phys.* **2008**, *104*, 053512.
[29] F. P. Bundy, T. H. Hall, H. M. Strong, R. H. Wentorf, Jr, *Nature* **1955**, *176*, 51.
[30] Y. Zhang, C. Zang, H. Ma, Z. Liang, L. Zhou, S. Li, X. Jia, *Diamond Relat. Mater.* **2008**, *17*, 209.
[31] R. H. Wentorf, *J. Chem. Phys.* **1957**, *26*, 956.
[32] P. F. McMillan, *Nat. Mater.* **2002**, *1*, 19.
[33] A. R. Badzian, *Appl. Phys. Lett.* **1988**, *53*, 2495.
[34] V. L. Solozhenko, D. Andrault, G. Fiquet, M. Mezouar, D. C. Rubie, *Appl. Phys. Lett.* **2001**, *78*, 1385.
[35] V. L. Solozhenko, S. N. Dub, N. V. Novikov, *Diamond Relat. Mater.* **2001**, *10*, 2228.
[36] C. M. Sung, Diamond Technology Center of Norton Company, private communication **1984**.
[37] C.-M. Sung, M. Sung, *Mater. Chem. Phys.* **1996**, *43*, 1.
[38] A. Y. Liu, M. L. Cohen, *Science* **1989**, *245*, 841.
[39] S. V. Meschel, O. J. Kleppa, *Metall. Trans. A* **1993**, *24*, 947.
[40] H. J. McSkimin, W. L. Bond, *Phys. Rev.* **1957**, *105*, 116.
[41] J. Maynard, *Phys. Today* **1996**, *49*, 26.
[42] A. Migliori, J. Sarrao, *Resonant Ultrasound Spectroscopy*, Wiley, New York **1997**.
[43] M. B. Weinberger, S. H. Tolbert, A. Kavner, *Phys. Rev. Lett.* **2008**, *100*, 045506.
[44] J. Zhang, Y. Zhao, R. S. Hixson, G. T. Gray, Iii, L. Wang, W. Utsumi, S. Hiroyuki, H. Takanori, *Phys. Rev. B* **2008**, *78*, 054119.
[45] J. F. Shackelford, W. Alexander, *CRC Handbook of Materials Science & Engineering*, CRC Press, Boca Raton, FL **2001**.
[46] R. W. Cumberland, M. B. Weinberger, J. J. Gilman, S. M. Clark, S. H. Tolbert, R. B. Kaner, *J. Am. Chem. Soc.* **2005**, *127*, 7264.
[47] B. Aronsson, *Acta Chem. Scand.* **1963**, *17*, 2036.
[48] U. Burkhardt, V. Gurin, F. Haarmann, H. Borrmann, W. Schnelle, A. Yaresko, Y. Grin, *J. Solid State Chem.* **2004**, *177*, 389.
[49] J. M. Leger, J. Haines, M. Schmidt, J. P. Petitet, A. S. Pereira, J. A. H. daJornada, *Nature* **1996**, *383*, 401.
[50] H.-Y. Chung, J. M. Yang, S. H. Tolbert, R. B. Kaner, *J. Mater. Res.* **2008**, *23*, 1797.
[51] W. C. Oliver, G. M. Pharr, *J. Mater. Res.* **1992**, *7*, 1564.
[52] H. Gou, L. Hou, J. Zhang, H. Li, G. Sun, F. Gao, *Appl. Phys. Lett.* **2006**, *88*, 221904/1.
[53] J. C. Hay, E. Y. Sun, G. M. Pharr, P. F. Becher, K. B. Alexander, *J. Am. Ceram. Soc.* **1998**, *81*, 2661.
[54] X.-Q. Chen, C. L. Fu, M. Krcmar, G. S. Painter, *Phys. Rev. Lett.* **2008**, *100*, 196403/1.
[55] Z. Y. Chen, H. J. Xiang, J. Yang, J. G. Hou, Q. Zhu, *Phys. Rev. B* **2006**, *74*, 012102/1.
[56] M. Hebbache, L. Stuparevic, D. Zivkovic, *Solid State Commun.* **2006**, *139*, 227.
[57] S. Chiodo, H. J. Gotsis, N. Russo, E. Sicilia, *Chem. Phys. Lett.* **2006**, *425*, 311.
[58] X. Hao, Y. Xu, Z. Wu, D. Zhou, X. Liu, J. Meng, *J. Alloys Compd.* **2008**, *453*, 413.
[59] J. Yang, H. Sun, C. Chen, *J. Am. Chem. Soc.* **2008**, *130*, 7200.
[60] S. La Placa, B. Post, *Acta Crystallogr.* **1962**, *15*, 97.
[61] A. Vegas, L. A. Martinez-Cruz, A. Ramos-Gallardo, A. Romero, *Z. Kristallogr.* **1995**, *210*, 574.
[62] H.-Y. Chung, M. B. Weinberger, J. B. Levine, R. W. Cumberland, A. Kavner, J.-M. Yang, S. H. Tolbert, R. B. Kaner, *Science* **2007**, *316*, 436.
[63] D. He, Y. Zhao, L. Daemen, J. Qian, T. D. Shen, T. W. Zerda, *Appl. Phys. Lett.* **2002**, *81*, 643.
[64] H.-Y. Chung, M. B. Weinberger, J. B. Levine, R. W. Cumberland, A. Kavner, J.-M. Yang, S. H. Tolbert, R. B. Kaner, *Science* **2007**, *318*, 1550d.
[65] G. M. Amulele, M. H. Manghnani, M. Somayazulu, *J. Appl. Phys.* **2006**, *99*, 023522/1.
[66] D. He, S. R. Shieh, T. S. Duffy, *Phys. Rev. B* **2004**, *70*, 184121/1.
[67] B. Kiefer, S. R. Shieh, T. S. Duffy, T. Sekine, *Phys. Rev. B* **2005**, *72*, 014102/1.
[68] A. B. Lyashchenko, V. N. Paderno, V. B. Filippov, D. F. Borshchevskii, *Sverkhtverdye Mater.* **2006**, 79.

[69] S. Otani, T. Aizawa, Y. Ishizawa, *J. Alloys Compd.* **1997**, *252*, L19.
[70] R. F. Zhang, S. Veprek, A. S. Argon, *Appl. Phys. Lett.* **2007**, *91*, 201914/1.
[71] W. Zhou, H. Wu, T. Yildirim, *Phys. Rev. B* **2007**, *76*, 184113/1.
[72] Y. Liang, B. Zhang, *Phys. Rev. B* **2007**, *76*, 132101/1.
[73] X. F. Hao, Y. H. Xu, Z. J. Wu, D. F. Zhou, X. J. Liu, X. Q. Cao, J. Meng, *Phys. Rev. B* **2006**, *74*, 224112.
[74] X. F. Hao, Z. J. Wu, Y. H. Xu, D. F. Zhou, X. J. Liu, J. Meng, *J. Phys. Condens. Matter* **2007**, *19*, 196212.
[75] Y. X. Wang, *Appl. Phys. Lett.* **2007**, *91*, 101904/1.
[76] J. B. Levine, S. L. Nguyen, H. I. Rasool, J. A. Wright, S. E. Brown, R. B. Kaner, *J. Am. Chem. Soc.* **2008**, *130*, 16953.
[77] M. G. Kanatzidis, R. Pottgen, W. Jeitschko, *Angew. Chem. Int. Ed.* **2005**, *44*, 6996.
[78] S. Otani, *J. Ceram. Soc. Jpn.* **2000**, *108*, 955.
[79] S. Otani, Y. Xuan, Y. Yajima, T. Mori, *J. Alloys Compd.* **2003**, *361*, L1.
[80] I. Higashi, M. Kobayashi, S. Okada, K. Hamano, T. Lundstrom, *J. Cryst. Growth* **1993**, *128*, 1113.
[81] S. Okada, K. Kudou, I. Higashi, T. Lundstroem, *J. Cryst. Growth* **1993**, *128*, 1120.
[82] S. Okada, K. Kudou, T. Lundstrom, *Jpn. J. Appl. Phys. Part 1* **1995**, *34*, 226.
[83] S. Niemann, W. Jeitschko, *Z. Naturforsch. B* **1993**, *48*, 1767.
[84] I. Higashi, Y. Takahashi, T. Atoda, *J. Cryst. Growth* **1976**, *33*, 207.
[85] K. Nakano, H. Hayashi, T. Imura, *J. Cryst. Growth* **1974**, *24*, 679.
[86] E. O. Hall, *Proc. Phys. Soc. London Sect. B* **1951**, *64*, 747.
[87] N. J. Petch, *J. Iron Steel Inst. London* **1953**, *174*, 25.
[88] X. Hao, Y. Xu, Z. Wu, D. Zhou, X. Liu, X. Cao, J. Meng, *Phys. Rev. B* **2006**, *74*, 224112/1.
[89] G. Steinle-Neumann, L. Stixrude, R. E. Cohen, *Phys. Rev. B* **1999**, *60*, 791.
[90] M. B. Weinberger, J. B. Levine, H.-Y. Chung, R. W. Cumberland, H. I. Rasool, J.-M. Yang, R. B. Kaner, S. H. Tolbert, *Chem. Mater.* **2009**, *21*, 1915.
[91] R. Hill, *Proc. Phys. Soc. London* **1952**, *65*, 349.
[92] J. Qin, D. He, J. Wang, L. Fang, L. Lei, Y. Li, J. Hu, Z. Kou, Y. Bi, *Adv. Mater.* **2008**, *20*, 1.
[93] S. N. Tkachev, J. B. Levine, A. Kisliuk, A. P. Sokolov, S. Guo, J. T. Eng, R. B. Kaner, *Adv. Mater.* **2009**, *21*, 1.
[94] J. R. Sandercock, *Top. Appl. Phys.* **1982**, *51*, 173.
[95] A. Raveh, I. Zukerman, R. Shneck, R. Avni, I. Fried, *Surf. Coat. Technol.* **2007**, *201*, 6136.
[96] J. Patscheider, *MRS Bull.* **2003**, *28*, 180.
[97] H. G. Prengel, W. R. Pfouts, A. T. Santhanam, *Surf. Coat. Technol.* **1998**, *102*, 183.
[98] M. Chhowalla, H. E. Unalan, *Nat. Mater.* **2005**, *4*, 317.
[99] W. J. Zhang, I. Bello, Y. Lifshitz, S. T. Lee, *MRS Bull.* **2003**, *28*, 184.
[100] J. E. Sundgren, *Thin Solid Films* **1985**, *128*, 21.
[101] S. Veprek, M. G. J. Veprek-Heijman, P. Karvankova, J. Prochazka, *Thin Solid Films* **2005**, *476*, 1.
[102] A. Latini, J. V. Rau, D. Ferro, R. Teghil, V. R. Albertini, S. M. Barinov, *Chem. Mater.* **2008**, *20*, 4507.
[103] A. Iost, R. Bigot, *Surf. Coat. Technol.* **1996**, *80*, 117.
[104] B. Jonsson, S. Hogmark, *Thin Solid Films* **1984**, *114*, 257.
[105] A. M. Korsunsky, M. R. McGurk, S. J. Bull, T. F. Page, *Surf. Coat. Technol.* **1998**, *99*, 171.
[106] E. S. Puchi-Cabrera, *Surf. Coat. Technol.* **2002**, *160*, 177.
[107] J. V. Rau, A. Latini, A. Generosi, V. R. Albertini, D. Ferro, R. Teghil, S. M. Barinov, *Acta Mater.* **2009**, *57*, 673.
[108] R. A. Andrievski, *Int. J. Refract. Met. Hard Mater.* **2001**, *19*, 447.
[109] R. W. Cumberland, R. G. Blair, C. H. Wallace, T. K. Reynolds, R. B. Kaner, *J. Phys. Chem. B* **2001**, *105* 11922.
[110] Q. Gu, G. Krauss, W. Steurer, *Adv. Mater.* **2008**, *20*, 3620.
[111] R. J. Nelmes, J. S. Loveday, D. R. Allan, J. M. Besson, G. Hamel, P. Grima, S. Hull, *Phys. Rev. B* **1993**, *47*, 7668.
[112] P. A. Romans, M. P. Krug, *Acta Crystallogr.* **1966**, *20*, 313.
[113] M. Wang, Y. Li, T. Cui, Y. Ma, G. Zou, *Appl. Phys. Lett.* **2008**, *93* 101905.
[114] T. Lundström, I. Rosenberg, *J. Solid State Chem.* **1973**, *6*, 299.
[115] E. J. Felten, *J. Am. Chem. Soc.* **1956**, *78*, 5977.
[116] P. Rogl, E. Rudy, *J. Solid State Chem.* **1978**, *24*, 175.
[117] P. Rogl, H. Nowotny, F. Benesovs, *Monatsh. Chem.* **1970**, *101*, 850.
[118] P. Rogl, H. Nowotny, F. Benesovs, *Monatsh. Chem.* **1970**, *101*, 27.